EARTH SURFACE PROCESSES AND LANDFORMS, VOL. 18, 407–425 (1993)

ROLE OF *IN SITU* COSMOGENIC NUCLIDES ^{10}Be AND ^{26}Al IN THE STUDY OF DIVERSE GEOMORPHIC PROCESSES

K. NISHIIZUMI, C. P. KOHL AND J. R. ARNOLD
Department of Chemistry, University of California, San Diego, La Jolla, CA 92093-0317, U.S.A.
R. DORN
Department of Geography, Arizona State University, Tempe, AZ 85287-0104, U.S.A.
J. KLEIN, D. FINK AND R. MIDDLETON
Department of Physics, University of Pennsylvania, Philadelphia, PA 19104, U.S.A.
AND
D. LAL
Geological Research Division, Scripps Institute of Oceanography, University of California, San Diego, 9500 Gilman Drive, La Jolla, CA 92093-0220, U.S.A.

Received 27 March 1992

ABSTRACT

The central premises of applications of the *in situ* cosmogenic dating method for studying specific problems in geomorphology are outlined for simple and complex exposure settings. In the light of these general models, we discuss the information that can be derived about geomorphic processes, utilizing concentrations of *in situ* produced cosmogenic radionuclides ^{10}Be (half-life = 1·5 ma) and ^{26}Al (half-life = 0·7 ma) in a variety of geomorphic contexts: glacial polish and tills; meteorite impact craters; alluvial fans; paleo-beach ridges; marine terraces; sand dunes; and bedrock slopes. We also compare ^{10}Be–^{26}Al data with results obtained by other dating methods. We conclude that the technique of measuring *in situ* cosmic ray produced nuclides holds promise for quantitative studies of processes and time-scales in a wide range of geomorphological problems.

KEY WORDS Nuclear dating methods Cosmogenic nuclides ^{10}Be ^{26}Al Rock varnish Geomorphology Land processes Surface exposure dating Geochronology

INTRODUCTION

Two principal dating approaches used in geomorphic investigations involve sampling either of material in a stratigraphic context, or of material exposed at the surface of the earth. Stratigraphic techniques rely on a synsedimentary framework appropriate for dating by a variety of techniques including K–Ar, ^{14}C, tephrachronology, uranium-series, thermoluminescence and paleomagnetism. The measured 'date' constrains the age of the depositional event above and below the sample. Stratigraphic age control, however, is not always valuable for studying processes responsible for the formation of the present-day land surface.

The concept that cosmic rays produce nuclides *in situ* in terrestrial rocks was explored first by Davis and Schaeffer (1955) for ^{36}Cl. Lal and Peters (1967) and Lal (1988) review the nuclide production mechanisms and rates, and applications. In a recent paper, Dorn and Phillips (1991) placed dating using *in situ* cosmogenic nuclides within the general context of other surface exposure dating approaches, for example soils and weathering, dendrogeomorphology, rock varnish and lichenometry. One of their conclusions was that cosmogenic nuclides are inherently superior in most geomorphic circumstances, because their concentrations

0197–9337/93/050407–19$14.50

are based on physical processes that can be quantitatively related to time. Also, they are useful over the entire Quaternary. Other methods are based on biological and chemical variables that are difficult to control. A number of radionuclides are produced in surface terrestrial rocks in sufficient amounts to be measured with a high degree of accuracy by accelerator mass spectrometry (AMS); for a recent review, see Elmore and Phillips (1987). There has been a growing number of studies verifying earlier models that cosmogenic nuclides do build up in surface materials over time, including the radionuclides ^{10}Be and ^{26}Al (Nishiizumi *et al.*, 1986, 1989), ^{36}Cl (Phillips *et al.*, 1986; Zreda *et al.*, 1991), ^{14}C (Jull *et al.*, 1989), and the stable nuclides ^{3}He (Craig and Poreda, 1986; Kurz, 1986; Cerling, 1990) and ^{21}Ne (Marti and Craig, 1987; Graf *et al.*, 1990).

In the rush towards measuring new nuclides and discovering unique applications, however, no general model has been presented to explain how cosmogenic nuclides can be used in geomorphology. This paper attempts to sketch a general model, which is illustrated with new *in situ* ^{10}Be–^{26}Al measurements in different types of geomorphic situations; a number of these are from sites with prior age control.

BACKGROUND ON COSMIC RAY EXPOSURE HISTORY AND RECORD

The central basis of application of the *in situ* cosmogenic nuclide method in geomorphology is the continuous production of nuclides in terrestrial solids in a geometry-sensitive manner. The nuclide production rate within a solid, besides being dependent on the altitude and latitude, is also a function of the topography (geometry of exposure) as well as composition and density of the target material. Within a rock, the production rate decreases exponentially with depth. The absorption mean-free-path in common rock types is of the order of $\sim 150\ \mathrm{g\,cm^{-2}}$; about 50–60 cm in typical rocks. This is the distance in which the cosmic ray flux is reduced by a factor of '*e*', due to nuclear interactions which absorb the cosmic radiation energy.

The nuclide production rate depends on the chemical composition of the rock and its location. When these are known, the concentration depends only on (i) the half-life of the nuclide, (ii) the geometry of cosmic ray irradiation of the rock during the rock's exposure history, and (iii) the exposure duration. Implicit here is the assumption that the cosmogenic nuclide is retained quantitatively in the rock. These considerations form the central basis of application of cosmogenic nuclides in geomorphology.

NUCLIDE BUILD-UP IN DIFFERENT GEOMORPHIC SETTINGS

Even for the case of complete retention of an *in situ* cosmogenic nuclide, solids exposed to cosmic radiation at a given site would accumulate very different amounts of nuclides, depending on their temporal history of exposure geometry. The largest accumulation would be expected for a surface that has experienced no aggradation and no, or little, erosion. Deposition on a surface or erosion of surface material would lead to a change in the rate of build up of concentrations of the cosmogenic nuclides.

The simplest case would be of a static, non-evolving surface. The concentration of a radionuclide in the sample can be described by the following equation (Lal, 1988, 1991):

$$N = \frac{P}{\lambda}(1 - e^{-\lambda t}) \tag{1}$$

where N is the concentration of the radionuclide (atoms $\mathrm{g^{-1}}$), P is the production rate of the nuclide (atoms $\mathrm{g^{-1}\,a^{-1}}$), t is the cosmic ray exposure age and λ is the decay constant of the nuclide $= \ln 2/t_{1/2}$ (where $t_{1/2}$ is the half-life of the nuclide). 'Secular equilibrium' between production and disintegration is reached at about a few times the half-life of the radionuclide (for half-lives of useful nuclides, see Table I).

For a stable nuclide, the nuclide concentration increases linearly with time:

$$N = P \cdot t \tag{2}$$

where t is the cosmic ray exposure duration. Implicit here is the assumption that at the start of irradiation, $t = 0$ and $N = 0$.

If, however, exposure geometry is not fixed, for example due to surface erosion, the test point receives a changing cosmic ray flux as the upper surfaces erode away. Take the case of a quartz grain that is sampled

Table I. Principal *in situ* cosmogenic nuclides in geomorphology

Nuclide	Half-life	Principal target element(s) in rocks	Approximate production rate at sea-level* (atoms/g quartz)
Radioactive			
^{10}Be	1·5 ma	O (quartz); O, Mg (olivine)	6·0
^{14}C	5740 years	O	20·0
^{26}Al	0·71 ma	Si (quartz)	37·0
^{36}Cl	0·30 ma	Ca, K, Cl	†
Stable			
^{3}He	–	O, Si, Fe	75
^{21}Ne	–	Si (quartz); Mg, Si (olivine)	15

* For geomagnetic latitudes $\geq 50°$ (Lal, 1991)
† Quartz has no principal target element for production of ^{36}Cl by nuclear spallation; however, it can be produced by neutron capture in trace amounts of any occluded Cl in the quartz crystal

from a present-day surface. As the overlying material erodes, the cosmic ray flux and therefore the nuclide production rate would increase in this grain as less 'shielding' covers the sample. If the rate of erosion is constant over the time-scale of the nuclides under examination, this would lead to an exponential increase in cosmic ray flux at a given point. The cosmic ray flux increases by a factor of 'e' for an erosional loss of Λ (g cm^{-2}) of surface, where Λ is the absorption mean free path of cosmic radiation in the material.

A simple case is that of rock material exposed for the first time at $t = 0$, with no initial amounts of the radionuclide present. Crystalline rocks exposed by glacial erosion, for example, would fit the model in Equations 1 and 2. As a basis for discussion of the results reported in this paper, we present two additional equations. If the surface undergoes continuous and constant erosion or deposition, we obtain the following relations for the concentration of a radionuclide (Lal and Arnold, 1985; Lal, 1991):

Case 1. Uniform rate of erosion of a surface

$$N = \frac{P}{\lambda + \mu\varepsilon}[1 - e^{-(\lambda+\mu\varepsilon)t}] \tag{3}$$

Case 2. Uniform rate of deposition of material on a surface

$$N = \frac{P}{\lambda - \mu s}[e^{-\mu x} - e^{-\lambda x/s}] \tag{4}$$

where the symbols N, P and λ are as defined before, ε and s are the erosion and aggradation rates respectively. The rock or the soil density, ρ (g cm^{-3}) and the cosmic ray absorption mean free path Λ are related to the cosmic ray absorption coefficient, μ (cm^{-1}) by the relation: $\mu = \rho/\Lambda$. Note that in both Equations 3 and 4, P is the cosmogenic nuclide production rate at the surface, $x = 0$. In the case of constant erosion, the surface sampled is at $x = 0$, whereas in the case of a constant rate of aggradation, the formula applies to a depth x.

Besides the two cosmic ray parameters, P and μ, the application of Equation 3 involves a knowledge of two geomorphic parameters, the erosion rate (ε) and the exposure duration time (t). In the case of Equation 4, the only parameter is the aggradation rate, s. Therefore if, from geomorphological considerations, the irradiation history of a sample can be adequately described, one can derive the unknown geomorphic parameter(s).

We must hasten to add that Equations 1 and 2 are oversimplified: it has been assumed that the concentration of the nuclide was 'zero' at $t = 0$. This situation is often not met in practice, as will be elaborated in the next section. Alternatively, if we assume that an erosional surface has been eroding for a long enough time period to reach a steady state [$t \gg 1/(\lambda + \mu\varepsilon)$] between nuclide production and erosion,

Equation 3 becomes:

$$N = \frac{P}{\lambda + \mu\varepsilon} \tag{5}$$

$$\frac{N}{P} = \frac{1}{\lambda + \mu\varepsilon} = T_{\text{eff}} \tag{6}$$

Equation 5 assumes a uniform erosion rate, and any changes in erosion rate or episodic erosion will lead to incorrect modelling. The 'steady state' model of constant erosion has been presented earlier (Lal and Arnold, 1985), as have a number of hypothetical irradiation geometries, potentially relevant to geomorphology (Lal, 1991). The effective exposure age, T_{eff}, in this case is given by Equation 6, and the total duration of exposure, t, by Equation 3. This paper relates theoretical models to real-world geomorphic contexts and actual ^{10}Be and ^{26}Al measurements. As we will see from the examples discussed later (Figures 2 and 3 and Tables II–IV), both absolute ^{10}Be and ^{26}Al concentrations and their ratios provide important information on the geomorphic history of samples. Because of their different half-lives, the ratio is also a sensitive function of the exposure history of the sample; its application requires a knowledge of their relative production rates, not their absolute production rates (Lal and Arnold, 1985).

In plain geomorphic terms, cosmic rays interact with rocks to produce a time signal of nuclide concentrations. Figure 1 (Lal, 1991) illustrates the time scales that can be studied using cosmogenic nuclides with different half-lives ranging from the late Tertiary to late-Holocene. Unfortunately, time is not the only geomorphic parameter that is uncertain. (1) The geometry of the sample may have changed. For example, a large boulder may have rolled over during its life on the surface of a landform and a sample collected from what is now the top surface of a boulder may have once been shielded by the entire boulder. This would have the net effect of decreasing past nuclide production and providing too young an age. (2) The surface of a landform may have experienced appreciable erosion since the geomorphic event of interest. (3) The surface of a landform may have experienced deposition (and then erosion of the cover) since the geomorphic event of interest. (4) A clast may have a prior history of exposure at or close to the surface involving burial, and re-exposure.

How these and other geomorphic uncertainties are handled depends in part on how a geomorphologist interprets the morphostratigraphic relationships of landform history at a site. Radionuclides (even when they may have the ideal physical and chemical properties) cannot provide the dynamic exposure history of the

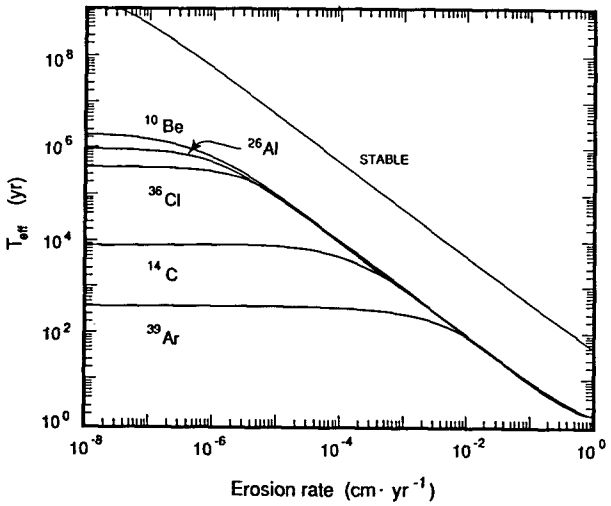

Figure 1. Calculated values of effective surface exposure ages (T_{eff}) as a function of erosion rate for five radionuclides and a stable nuclide (from Lal, 1991)

sample unless, based on the geomorphological context, one can utilize an appropriate exposure-history model. Here lies the crux of geomorphic studies using the *in situ* cosmogenic nuclides. This is what we would like to consider in some detail, with the backdrop of model calculations centring around Equations 1 to 5.

In the next sections we briefly discuss the experimental procedures for studies of cosmogenic radionuclides and then present results of measurements of concentrations of *in situ* cosmogenic ^{10}Be and ^{26}Al in samples studied from a variety of geomorphic situations.

EXPERIMENTAL METHODS

The selection of samples in the field was made primarily on the basis of their importance in different geomorphic contexts, as well as on their earlier characterization in other studies.

In this and earlier work, quartz was separated from various surface materials and purified by selective chemical dissolution (Kohl and Nishiizumi, 1992). Subsequently, 15–125 g of purified quartz were dissolved in HF with 1·5 mg of Be carrier. The chemical procedures for separation and purification of ^{10}Be and ^{26}Al from quartz are described by Kohl and Nishiizumi (1992). The ^{10}Be and ^{26}Al measurements were performed on the University of Pennsylvania's FN tandem van de Graaff accelerator (Klein *et al.*, 1982; Middleton *et al.*, 1983). Measured isotopic ratios were corrected for blank and background, and normalized to their respective standards. All standards were prepared in La Jolla and were those used for previous AMS measurements.

For comparison in Table II, we also include previous measurements of varnish radiocarbon ages. A radiocarbon age of rock varnish dates the time when bits of organic detritus were encapsulated by accreting varnish (Dorn, 1989; Dorn *et al.*, 1992). At best, a rock varnish age measures an event, the beginning of deposition of 'contemporary' ^{14}C in the varnished layer depositing on an exposed surface. One seeks to select specimens on which this basal layer can be unambiguously identified and sampled. Details on sample preparation for ^{14}C can be found in Dorn *et al.* (1992).

Cation ratio (CR) dating of varnish is less certain. It relies on a calibration of the ratio $(K^+ + Ca^{2+})/Ti^{4+}$ with reference to established numerical ages (Dorn, 1989). Recent advances have established that leaching is the mechanism of CR change over time (Dorn and Krinsley, 1991).

An important distinction between the rock varnish ages and the ^{10}Be–^{26}Al ages is that between methods which ideally record an event (standard ^{14}C dating) and methods which measure the duration of an interval, such as the integrated surface exposure (based on *in situ* cosmogenic ^{10}Be–^{26}Al in quartz). Another important difference is that whereas the rock varnish is removed by the erosion of the very skin (<1 mm) of a rock, the cosmogenic nuclides are not, since the cosmic ray particles have an absorption mean-free-path on the order of 50–60 cm in typical rocks. We view the cosmogenic approach as complementary to dating of rock coatings such as the rock varnish method. A varnish age measures a point in time after the last erosional event. Cosmogenic nuclides, in contrast, integrate time in the upper 50–60 cm; they provide approximately the 'dwell time' of the sample in the upper 50–60 cm layer.

RESULTS IN DIFFERENT GEOMORPHIC CONTEXTS

In the light of the foregoing we will now discuss the diverse geomorphic samples studied for cosmogenic ^{10}Be and ^{26}Al, in order of increasing complexity.

Case study of glacial polish: no prior exposure history and no erosion

Consider a stoss and lee glacial landform. Following removal by glacial processes, a polished bedrock surface remains and provides an example of a static, non-eroding surface. A stable cosmogenic nuclide (^{3}He, ^{21}Ne) would accumulate continuously, linearly with time, according to Equation 2. For radionuclides with both build-up and decay, their concentration would build up to the secular equilibrium value (Equation 1 with $t \gg t_{1/2}$).

A reasonable assumption is that the glacier has removed enough of an overburden of rock to expose the polished rock to cosmic rays for practically the first time; i.e. $N = 0$ at $t = 0$. This assumption is easily tested by comparing the 'exposure age' of a stable nuclide with that for a radionuclide. If the surface had been

Table II. ^{10}Be and ^{26}Al concentrations and exposure ages

Site	Sample	Lat. (°)	Long (°)	Alt. (m)	Al (ppm)	^{10}Be (10^6 atom/g SiO_2)	^{26}Al (10^6 atom/g SiO_2)	Minimum exposure age (ka)	Varnish ^{14}C age† (ka)
Pine Creek glacial till	Tioga Glaciation Site 1*	37·4 N	118·6 W	1890	37	0·29 ± 0·02	1·90 ± 0·17	13·8 ± 0·8	13·17 ± 0·10
	Tioga Glaciation Site 2*	37·4 N	118·6 W	1876	50	0·27 ± 0·02	2·05 ± 0·09	13·9 ± 2·4	13·91 ± 0·21
	Tioga Glaciation Site 3*	37·4 N	118·6 W	1743	42	0·37 ± 0·02	2·00 ± 0·10	17·5 ± 1·2	19·05 ± 0·42
	Rovana Glac. Site 5*	37·4 N	118·6 W	1609	59	1·76 ± 0·09	9·79 ± 0·42	95 ± 4	
	Rovana Glac. Site 6*	37·4 N	118·6 W	1585	43	1·94 ± 0·10	12·2 ± 0·6	115 ± 6	
White Mountain glacial moraines	Chiatovich P8	37·8 N	118·3 W	2810	–	0·70 ± 0·04	4·08 ± 0·29	17·5 ± 0·8	‡
	Chiatovich P23	37·8 N	118·3 W	2950	–	0·58 ± 0·03	3·42 ± 0·015	13·3 ± 0·5	‡
	Chiatovich P9	37·8 N	118·3 W	3050	–	2·19 ± 0·11	14·69 ± 0·88	51 ± 4	‡
	Chiatovich P25	37·8 N	118·3 W	2260	–	3·41 ± 0·16	17·6 ± 1·1	116 ± 11	‡
	Cottonwood Erratic	37·5 N	118·2 W	3595	–	9·28 ± 0·43	53·8 ± 2·6	155 ± 5	‡
	Dyer Till	37·5 N	118·1 W	1760	–	1·45 ± 0·08	8·12 ± 0·43	71 ± 3	‡
Death Valley alluvial fans	Hanaupah Cyn Unit 3a*	36·4 N	117·0 W	300	152	0·77 ± 0·04	4·72 ± 0·25	117 ± 4	> 43
	Hanaupah Cyn Unit 2a*	36·4 N	117·0 W	300	201	1·65 ± 0·08	9·71 ± 0·41	260 ± 9	
	Hanaupah Cyn Unit 1a*	36·4 N	117·0 W	300	20	1·91 ± 0·10	11·7 ± 0·4	314 ± 22	
	Galena Cyn Unit 2a*	36·4 N	117·0 W	300	436	2·00 ± 0·13	11·4 ± 0·4	318 ± 12	
	Galena Cyn Unit 1b*	36·4 N	117·0 W	300	40	2·03 ± 0·08	11·9 ± 1·4	320 ± 14	

Bedrock	Cliff Face	38·5 N	114·0 W	1859	182	0·12 ± 0·01	0·82 ± 0·05	10·8 ± 1·3	‡
	Wingate SS, UT								
	Himalaya-56 China	32·9 N	79·8 E	4750	135	4·73 ± 0·50	18·8 ± 3·1	41 ± 12	na
	Himalaya-80 China	33·5 N	79·0 E	4500	45	0·87 ± 0·16	5·18 ± 0·68	9·8 ± 1·1	na
	Mt. Evans Colorado	39·6 N	105·6 W	4298	20	6·29 ± 0·30	34·4 ± 1·2	66 ± 4	na
	Grand Teton Wyoming	33·7 N	110·5 W	4199	70	1·28 ± 0·14	5·89 ± 0·61	13·7 ± 2·2	na
Littoral	Manix Lake	35·0 N	119·0 W	543	21	0·43 ± 0·02	2·63 ± 0·21	54 ± 2	13·97 ± 0·12 §
	Beach Ridge S. Peru	14·5 S	75·5 W	300	85	1·08 ± 0·05	5·37 ± 0·20	280 ± 29	na
	Marine Terrace S. Peru	14·5 S	75·5 W	20	186	0·59 ± 0·03	2·62 ± 0·11	112 ± 23	na
	Marine Terrace S. Carolina	33·0 N	81·4 W	70	23	1·17 ± 0·06	7·97 ± 0·53	312 ± 56	na
	Upland Unit S. Carolina	33·0 N	81·4 W	70	393	2·53 ± 0·12	8·51 ± 0·40	408 ± 160	na
	Upland Unit								

* Site numbers correspond to Figures 4 and 6
† Varnish ages are previously published for Pine Creek (Dorn *et al.*, 1987; Dorn *et al.*, 1990), Death Valley (Dorn, 1988; Dorn *et al.*, 1989) and Manix Lake (Dorn *et al.*, 1989)
‡ Results in progress
§ Radiocarbon date on *Anodonta* shells 14·2 ± 1·3 ka (Meek, 1989)
na = not available

'repolished' by a later glaciation, removing only a few centimetres of material, the stable nuclide production would be from multiple exposures, while the radionuclide would have decayed when the glacier was present over the site. In contrast, if the glacially polished surface had experienced cosmic ray bombardment only since the last deglaciation, the stable and radionuclide ages would coincide. Published case studies of glacial polish provide examples of both situations.

Nishiizumi *et al.* (1989) measured ^{10}Be–^{26}Al in glacially polished samples from the Sierra Nevada, California. The concentrations of ^{10}Be and ^{26}Al are consistent with what is known about the timing of the last major deglaciation of the Sierra nevada from radiocarbon measurements — that deglaciation occurred around 10–14 ka BP. About a dozen rock surfaces with glacial polish, from altitudes of 2060–3560 m and different exposure geometries yielded consistent accumulation rates of ^{10}Be and ^{26}Al in quartz. These studies have unambiguously demonstrated on the one hand, that accumulation of a cosmogenic nuclide can be used in geomorphology, and on the other hand, that nuclide production rates can be estimated directly from studies of well documented geomorphic samples.

Figure 2 displays how a surface of glacial polish would record the build-up of ^{26}Al and ^{10}Be. In this plot of ^{26}Al/^{10}Be ratios vs. ^{10}Be and ^{26}Al concentrations over time (Nishiizumi *et al.*, 1991a), the upper curves in

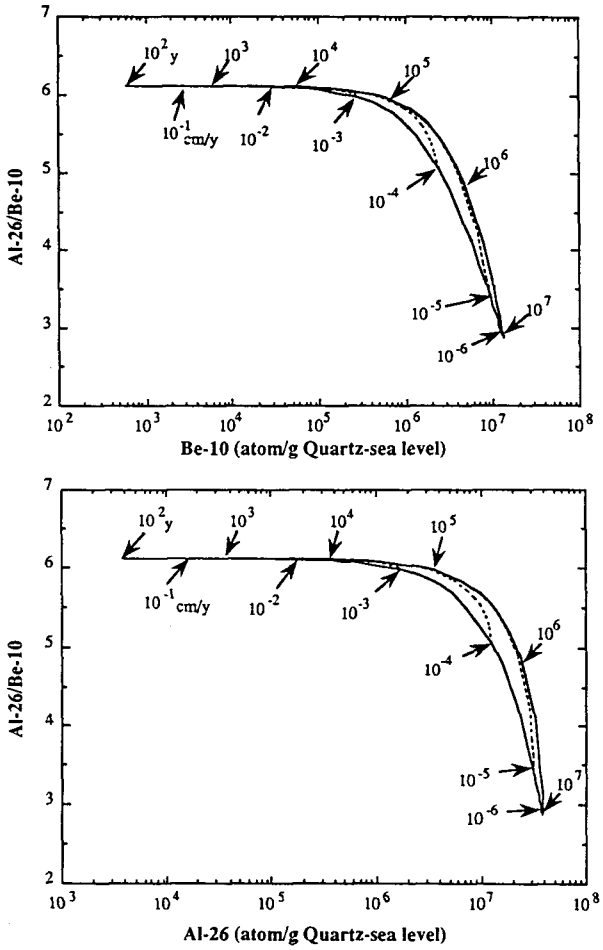

Figure 2. (a) ^{10}Be and (b) ^{26}Al concentrations (normalized for atom/g of quartz at sea level) plotted against ^{26}Al/^{10}Be ratios. The upper curves are calculated for zero erosion with different 'exposure ages' as shown. The bottom curves are calculated for different erosion rates. The dotted lines show the 'progress' of three different exposure histories with material undergoing 'constant erosion' (10^{-3}, 10^{-4} and 10^{-5} cm a^{-1}) after starting with specific finite ages 10^4, 10^5 and 10^6 years respectively (from Nishiizumi *et al.*, 1991a).

each graph display expected values under the condition of zero erosion of the glacial polish. For about the first 10^5 years $^{26}Al/^{10}Be$ ratios remain close to their value at production, at about 6. Since ^{26}Al approaches secular equilibrium before ^{10}Be, the concentration of ^{10}Be continues to increase until it too reaches secular equilibrium at the lower right corner of the diagram, at a ratio close to 3.

Case studies of low erosion rock surfaces

In Figure 2 (Nishiizumi *et al.*, 1991a), the lower curves on each graph present the case of constant erosion, which we acknowledge is a very unlikely way for a landscape to behave. Yet, it exemplifies the potential of measuring multiple nuclides. At higher rates of surface erosion ($\sim 10^{-1}$ to 10^{-3} cm a^{-1}), $^{26}Al/^{10}Be$ ratios remain similar. As erosion rates decrease, the $^{26}Al/^{10}Be$ ratios decrease significantly. The 'island' that is created between the zero erosion and constant erosion lines in Figure 3 is termed the 'steady state erosion island' (Lal, 1991).

About 20 samples of rocks were collected from surfaces at various locations in Antarctica (Nishiizumi *et al.*, 1991a). Figure 3 shows results for seven samples collected at Sör Rondane, Antarctica. A few samples had near-saturation accumulation of ^{26}Al and ^{10}Be, indicated by their position in the lower right corner on a plot of $^{26}Al/^{10}Be$ vs. ^{10}Be (Figure 3). Most of these samples plot on or close to the steady-state erosion line expected for continuous erosion (Lal, 1991; Nishiizumi *et al.*, 1991a). The maximum erosion rates of > 95 per cent of the Antarctic samples which were studied lie in the range 10^{-5}–10^{-6} cm a^{-1} (Table III). This corresponds to an effective surface-exposure age of 5×10^5 to $> 3 \times 10^6$ years. Samples 8 and 9 plot well below the erosion island, indicating burial (or ice cover) for a length of time; lower $^{26}Al/^{10}Be$ ratios in samples 8 and 9 arise due to the relatively higher rate of decay of ^{26}Al (Table I) than ^{10}Be.

A contentious issue in geomorphology has been long-term rates of geomorphic activity. The observations on the Sierra and the Antarctic rocks demonstrate the efficacy of the *in situ* cosmogenic nuclides for the study of low rates of erosion. On the southeastern edge of the Australian continent, Young (1983) used K–Ar dated lava flows as a base-line to assess the tempo of geomorphic change. He concluded that these terrains have been stable for an exceptionally long time. Results on cosmogenic exposure ages of sands and bedrock surfaces from a variety of areas in Australia (Nishiizumi *et al.*, 1992) also show extremely long ages and point to stable landforms. Indeed the Australian continent is second only to Antarctica in what have now been recognized as sites of long duration of bedrock surface exposure. These measurements certainly support the perspective that at least some parts of the earth's surface have changed little over millions of years due to the low erosion rates prevalent there, as determined for the first time.

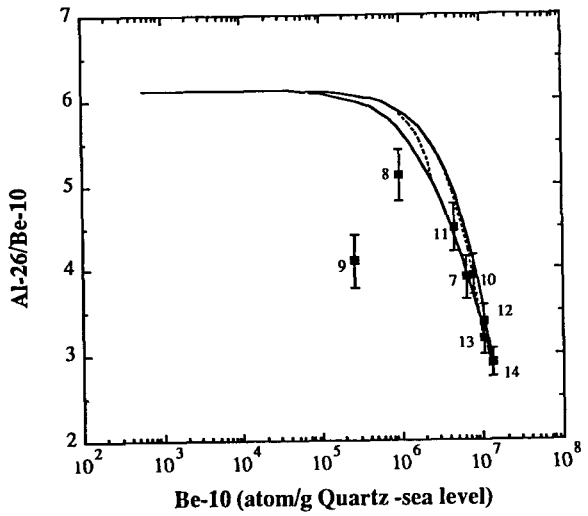

Figure 3. ^{10}Be concentrations (normalized for atom/g quartz at sea level) plotted against $^{26}Al/^{10}Be$ ratios for Sör Rondane samples from Antarctica (from Nishiizumi *et al.*, 1991a; see this reference for numbers which refer to different samples)

Table III. Sherwin Till ^{10}Be and ^{26}Al concentrations (data from Nishiizumi *et al.*, 1989)

Sample code	Depth below tuff bottom layer (cm)	Concentrations (atoms g^{-1})*		
		^{10}Be	^{26}Al	$^{26}Al/^{10}Be$
W86-19	0–4	1·028 ± 0·066	5·03 ± 0·26	4·90 ± 0·40
W86-18-2	15–20	1·165 ± 0·162	–	–
W86-18	15–20	1·094 ± 0·006	–	–
W86-17	35–45	1·310 ± 0·11	5·67 ± 0·32	4·33 ± 0·43

* Values are corrected for 730 000 years of decay for Bishop Tuff (cf. Sharp, 1968)

Case study of shielded rocks exposed in a sudden event: meteorite impact

Excavation of rock by formation of an impact crater is one example of exposure during a sudden event. In this case it should be possible to obtain the age of the event if the material sampled originated from a great enough depth to be considered shielded from cosmic radiation. Of course there will be some erosion of the rocks and the ages obtained will be minimum ages. But if the exposure is relatively short, the amount of erosion and the correction will be small. We have demonstrated such an age determination for Meteor Crater, Arizona (Nishiizumi *et al.*, 1991b). The age obtained is 49 200 ± 1700 years, based on exposure ages of the five large ejecta blocks sampled. It is in good agreement with the age determined by Phillips *et al.* (1991) based on ^{36}Cl measurements from samples taken at many of the same locations. This age reflects the exposure time since the removal of the fallout layer which must have covered these blocks to an indeterminate depth just after the impact.

A special study (Nishiizumi *et al.*, 1991b) was carried out to measure the present-day denudation rate for comparison with the earlier rates. It is important to note here that it is the denudation rate of the soil that is being investigated and not the erosion rate of the rock. Measurements of ^{10}Be and ^{26}Al concentrations in a sample from the side of one of the ejecta blocks compared with measurement from the top of the block gives denudation rates of 5 cm/1000 a for the last 23 000 years and 30 cm/1000 a during the period from 49 000 to 27 000 years ago. Evidently, denudation rates were highest shortly after the crater formed. On the basis of these values and other geological evidence it seems that the top of the large ejecta blocks sampled for this study may have been exposed within a few thousand years of the formation of the crater.

Case study of accumulation

A large number of geomorphological problems involve an aggrading surface. In many contexts, charcoal for radiocarbon dating is available. In other circumstances, no suitable material is available for dating, or the time range is inappropriate, or the investigator wishes to know how long the surface (now buried) was formerly exposed. This is the case for the Sherwin Till, which was buried beneath the Bishop Tuff in the eastern Sierra Nevada, California, about 0·73 ma BP.

Nishiizumi *et al.* (1989) measured ^{10}Be and ^{26}Al concentrations in samples from the Sherwin Till, a morainal deposit exposed in many places on the eastern slope of the Sierra (37·6° N, 2060 m). However, in a road cut on highway 395, it is buried below an extensive and thick (tens of metres) welded tuff deposit, designated the Bishop Tuff.

In the Sherwin Till at this site, all the *in situ* production occurred before the ash layer was deposited, since the cosmic ray production was reduced to a minimal value immediately after the emplacement of the thick tuff. The ^{10}Be concentrations in the till increase with depth, as would also be theoretically expected (Equation 4); see also Lal *et al.* (1987) for *in situ* production of ^{14}C and ^{10}Be in accumulating ice. This can be explained by a slow rate of deposition for the till at this location (Table III). If we assume a zero initial ^{10}Be concentration for the aggrading material, then the ^{10}Be and ^{26}Al concentrations (Table III) are consistent with an aggradation rate of $\sim 10^{-3}$ cm a^{-1}. If, however, the initial ^{10}Be concentration is taken as $\leqq 0{\cdot}2\times$

the observed value, then the aggradation rate is estimated to be $< 3 \times 10^{-3}$ cm a^{-1}. Measurements at greater depths in the Sherwin Till (in progress) would constrain rates of till deposition more closely.

We have thus seen that the measurement of cosmogenic nuclides in buried geomorphic surfaces has great potential, provided an appropriate model is used. In the absence of a good working model, one would have to make detailed analyses of the *in situ* nuclides as a function of depth, to constrain the model.

Case study of glacial moraines: Pine Creek

Glacial moraines add another degree of complexity, because some of the boulders could have potentially experienced a significant prior exposure before being eroded, transported by the glacier and deposited. Also, the geometry of a glacial boulder sampled from a moraine crest may have changed, for example, by rolling or by rotating. Lastly, arguments can ensue about the rates of erosion of the surface glacial boulders and moraines themselves.

Figure 4 presents a photograph of the glacial moraines at Pine Creek, eastern Sierra Nevada in California, with sampling sites indicated by numbers corresponding to Table II. Sample Tioga site 2 was collected by Cerling (1990). The other samples were collected by Dorn. Pine Creek has been studied by Bateman (1965), Dorn *et al.* (1987, 1990), Bach *et al.* (1991) and Berry (1991). Table II presents ^{10}Be–^{26}Al exposure ages assuming no boulder geometry changes, no surface erosion and no prior exposure history.

Pine Creek is an appropriate site to explore the dating of deposits like glacial till, because of the abundance of prior age control. A radiocarbon date is available for organics sampled from the till matrix; 19·5 ka for a Tioga moraine that is correlative with 'Tioga' site 3 (Bach *et al.*, 1991).

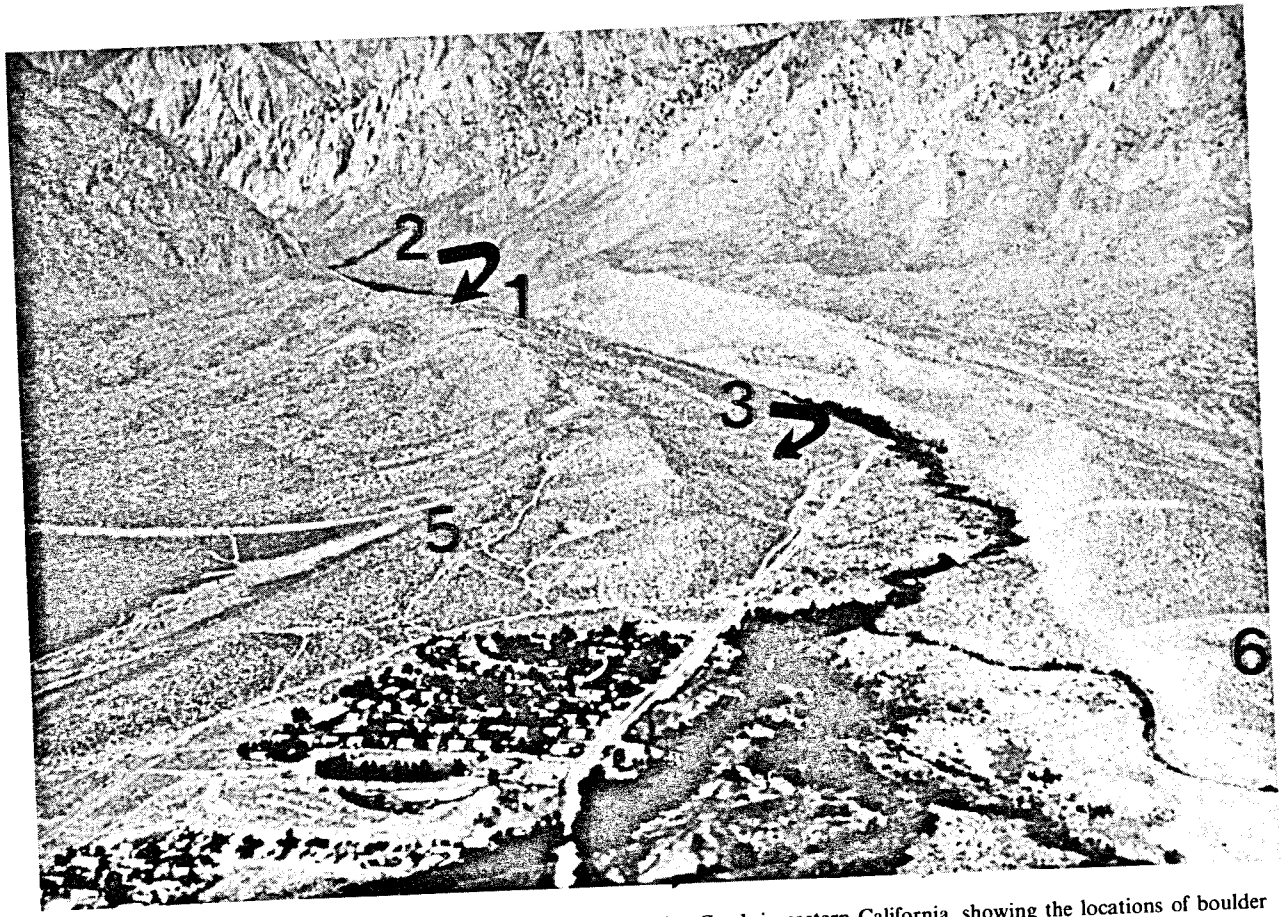

Figure 4. Oblique aerial photograph of the glacial moraines at Pine Creek in eastern California, showing the locations of boulder collection. Sample numbers correspond to data in Table II

The same boulders sampled for ^{10}Be–^{26}Al concentrations were also sampled for varnish dating at all sites except the Tioga site 2, and these data are found in Table II. As was mentioned, varnish dating provides a different type of information from the cosmogenic nuclides; the ages provide only a minimum-limiting age for exposure of the underlying rock. A varnish age is not sensitive to changes in boulder geometry, but the varnish clock is reset by even a millimetre of surface erosion.

The most conservative interpretation for the ^{10}Be–^{26}Al data from Pine Creek is that the exposure ages in Table II are minima, due to possibilities of boulder erosion, boulder rotation, and moraine crest degradation. Still, numerical ages, even minima, are a great improvement in resolution over relative ages based on weathering and soil characteristics. The conventional radiocarbon age on a Tioga moraine equivalent to b1, and varnish ages for a series of Tioga moraines sites 3, 2 and 1 coincide with the ^{10}Be–^{26}Al ages, which suggests that the sampled boulders have not changed their geometry significantly, that they had not experienced a prior exposure history and that the surface of the boulders has not eroded to a significant extent.

Case study of eroding bedrock exposures

Figure 5 presents a cliff face of Wingate Sandstone at Islands in the Sky of Canyonlands National Park in Utah. As can be seen in the photograph, the cliff face erodes by slab failure, where the thickness of the slabs varies. Position 2 in the photograph is where the ^{10}Be–^{26}Al sample was collected (Table II). It is likely that the slab which is about 70 cm thick at position 1 once covered the site at position 2. Therefore, this site can be

Figure 5. Cliff face on Wingate Sandstone at Islands in the Sky, Utah. The sample with a ^{10}Be–^{26}Al exposure history of about 8–9 ka was collected from position 2. There used to be a cover of about 70 cm, as evidenced by the slab of sandstone at position 1. Failure at this point on the cliff appears to be by spalling of this massive slab

modelled somewhere between slab failure creating a surface with no prior exposure history and continuous granular erosion.

If a correction is applied for the vertical cliff face, but not for some earlier penetration of cosmic rays through the covering ~70 cm slab at position 1, an apparent exposure age is obtained in Table II of about 10–11 ka. When we measure the ^{10}Be–^{26}Al concentrations at position 1, we may be able to constrain the prior exposure history and provide a more accurate age for slab failure, and also possibly obtain ages for successive cliff positions, and thus provide estimated rates of cliff retreat. Although we have only a single data point from a site that requires further study, a conservative interpretation of the ^{10}Be–^{26}Al exposure age demonstrates that sandstone cliffs in the Colorado Plateau can maintain vertical faces for thousands of years—a useful insight.

In our studies, we admit to the bias of trying to sample the most stable surfaces. Since sampling procedures are still intuitive, we have looked for remnants of 'original surfaces'. The search for stability has yielded remarkably stable surfaces in Antarctica (Table IV). Samples from the Sör Rondane mountains in Antarctica show very low erosion rates.

On the other hand, samples from exposed bedrock in the Himalayas, the Teton Range, and Borrego distinctly show erosion rates about two orders of magnitude higher than the Antarctic rocks (Table IV). The Himalayan samples are grandodiorite collected by G. Teying. Himalaya-56 is from north of Shiqianhe and 80 is from south of Ritu county; both samples are from the Gongdis belt. They were collected for us with erosion studies in mind. Sampling requests specified a nearly horizontal, surface bedrock sample open to the full sky cosmic ray exposure. There are no photographs of these *in situ* samples. There is the possibility of an intermittent snow cover for 3–4 months of the year. The Grand Teton granodiorite was collected by J. Hawkins from a slightly inclined surface near the summit of the Grand Tetons. The Mt. Evans, Colorado granite was collected by us from near the A frame at the summit of the mountain from the top of a boulder. This site experiences high winds and we expect no significant snow cover. The sample location is adjacent to the site of our target experiment to determine production rates of ^{10}Be, ^{26}Al, and ^{21}Ne in Si, Mg and SiO_2.

The ability to obtain numerical ages for bedrock exposures opens up new horizons for the analysis of geomorphic situations that were previously impossible to assess in a quantitative manner. The erosion rate is

Table IV. Maximum erosion rates of bedrock sampled from Antarctica, compared to bedrock erosion in other terrestrial settings

	Antarctic rocks			
Erosion bracket ($cm\,a^{-1}$)	Allan Hills	Sör Rondane	Wright Valley	Others rocks*
$1–2 \times 10^{-6}$				
$2–4 \times 10^{-6}$		1		
$4–8 \times 10^{-6}$		2		
$0{\cdot}8–1{\cdot}6 \times 10^{-5}$				
$1{\cdot}6–3{\cdot}2 \times 10^{-5}$	1	2		
$3{\cdot}2–6{\cdot}4 \times 10^{-5}$	4	1	1	
$0{\cdot}64–1{\cdot}28 \times 10^{-4}$	3		2	
$1{\cdot}28–2{\cdot}56 \times 10^{-4}$	2		1	
$2{\cdot}56–5{\cdot}12 \times 10^{-4}$				
$0{\cdot}51–1{\cdot}02 \times 10^{-3}$				
$1{\cdot}02–2{\cdot}05 \times 10^{-3}$				1 (E)
$2{\cdot}05–4{\cdot}1 \times 10^{-3}$				2 (B, H)
$4{\cdot}1–8{\cdot}2 \times 10^{-3}$				1 (B)
$0{\cdot}82–1{\cdot}6 \times 10^{-2}$				2 (GT, H)

*E = Mt. Evans, Colorado; B = Anza Borrego, California; H = Himalayas; GT = Grand Tetons, Wyoming

calculated to be $1{\cdot}4 \times 10^{-3}$ cm a^{-1} for Himalaya-56, $5{\cdot}6 \times 10^{-3}$ cm a^{-1} for Himalaya-80, $8{\cdot}2 \times 10^{-4}$ cm a^{-1} for Mt. Evans and $4{\cdot}8 \times 10^{-3}$ cm a^{-1} for Grand Teton.

Case study of a Paleo-Beach Ridge

About 10 quartzite pebbles collected from the large beach ridge at the east end of Pleistocene Lake Mannix were combined for ^{10}Be–^{26}Al measurements. A full description of the collection site can be found in Meek (1989). The radiocarbon ages are $14{\cdot}2 \pm 1{\cdot}3$ ka for Anodonta shells (Meek, 1989), and $13{\cdot}9 \pm 0{\cdot}1$ ka for rock varnish (Dorn *et al.*, 1989). Yet the apparent ^{10}Be–^{26}Al ages are ~54–55 ka, assuming the pebbles processed remained at the surface. This is not a contradiction, but expected from conceptual geomorphic models of the formation of beach ridges. The clasts in the beach ridge were exposed once on a hillslope, then transported in a fluvial system for probably a few kilometres, further transported in the littoral zone of Lake Mannix, and finally deposited on top of the beach ridge. The beach ridge was abandoned when Lake Mannix was breached, probably in a catastrophic fashion.

The ~40 ka difference between the ^{10}Be–^{26}Al exposure ages and the age of the beach ridge includes both the hillslope exposure and the exposure during transport. A hillslope–fluvial transport time for these pebbles is about 40 ka, assuming constant exposure at the surface. Since transport was probably not at the surface, this is a minimum estimate for how long it takes individual clasts to move in this hillslope → fluvial → lacustrine transport path.

This is the first example of the long-term transport rates of individual pebbles. This type of approach opens the door to assessing the representativeness of present-day studies of pebble transport. When the age of the landform at the end-point of the system is established, it is possible to constrain the long-term transport history of clasts at different points along the way. Studies of other cosmogenic nuclides, the shorter half-life nuclide ^{14}C and the stable nuclide ^{21}Ne, would further constrain the history of the clasts.

Case study of alluvial fans in Death Valley

We would expect clasts in alluvial fans to represent examples of complex prior exposure history. Clasts would first experience exposure under a cover on a slope, then exposure as the overburden erodes, then hillslope transport at the surface or at depth, then transport to a fan unit and perhaps erosion and redeposition on a fan unit, and lastly erosion of the clast on a surface.

The bajada on the east side of the Panamint Range is a classic site for the study of alluvial fans in drylands (e.g. Dorn, 1988; Harvey, 1989). Samples from Hanaupah Canyon and Galena Canyon fans in Death Valley, previously collected for radiocarbon dating on organics, radiocarbon dating on calcrete rinds, and varnish age determination, were selected for ^{10}Be–^{26}Al dating. Figure 6 shows the locations of the samples discussed below. Table II shows the results.

The age of the Q3a unit (unit identification in Dorn, 1988) on the Hanaupah fan is the best constrained. For the ^{10}Be–^{26}Al sampled boulder on Q3a (minimum apparent exposure age of 117 ± 4 ka), the varnish radiocarbon age is infinite (>43 000; AA-1416). Soil development at this site has produced ~40 mm thick calcrete rinds, but an argillic B horizon has not developed (Stadelman, 1989). A ^{14}C age on organic matter extracted from an inner calcrete rind at this site is also infinite (>37 000). While these dead radiocarbon ages are consistent with the ^{10}Be–^{26}Al exposure age, a radiocarbon age of $23\,420 \pm 550$ years is available for a site down-fan on the same Q3a unit of Hanaupah Canyon Fan on charcoal collected just under the surface. (This part of the fan is also associated with a varnish radiocarbon age of $21\,740 \pm 280$ years; a ^{14}C age of $17\,570 \pm 145$ years on organic matter extracted from an inner calcrete rind; and a ^{14}C age of $21\,235 \pm 175$ years on an inorganic inner calcrete rind.)

The exposure period of $>117 \pm 4$ ka for Q3a could and probably does represent two or more exposure intervals. The ^{26}Al/^{10}Be ratio, close to 6, constrains all significant exposures to a total interval $<5 \times 10^5$ years.

The minimum apparent exposure age of the Q2a unit is 260 ka. The only other radioactive age estimate for the Q2a unit are uranium-series ages of ~112 ka and ~178 ka on calcrete rinds from Johnson Canyon fan (Hooke and Lively, 1979). The relation of these dates is not clear. Both the varnish and the calcrete age signals are reset by abrasive transportation, but the ^{10}Be–^{26}Al accumulation is not reset.

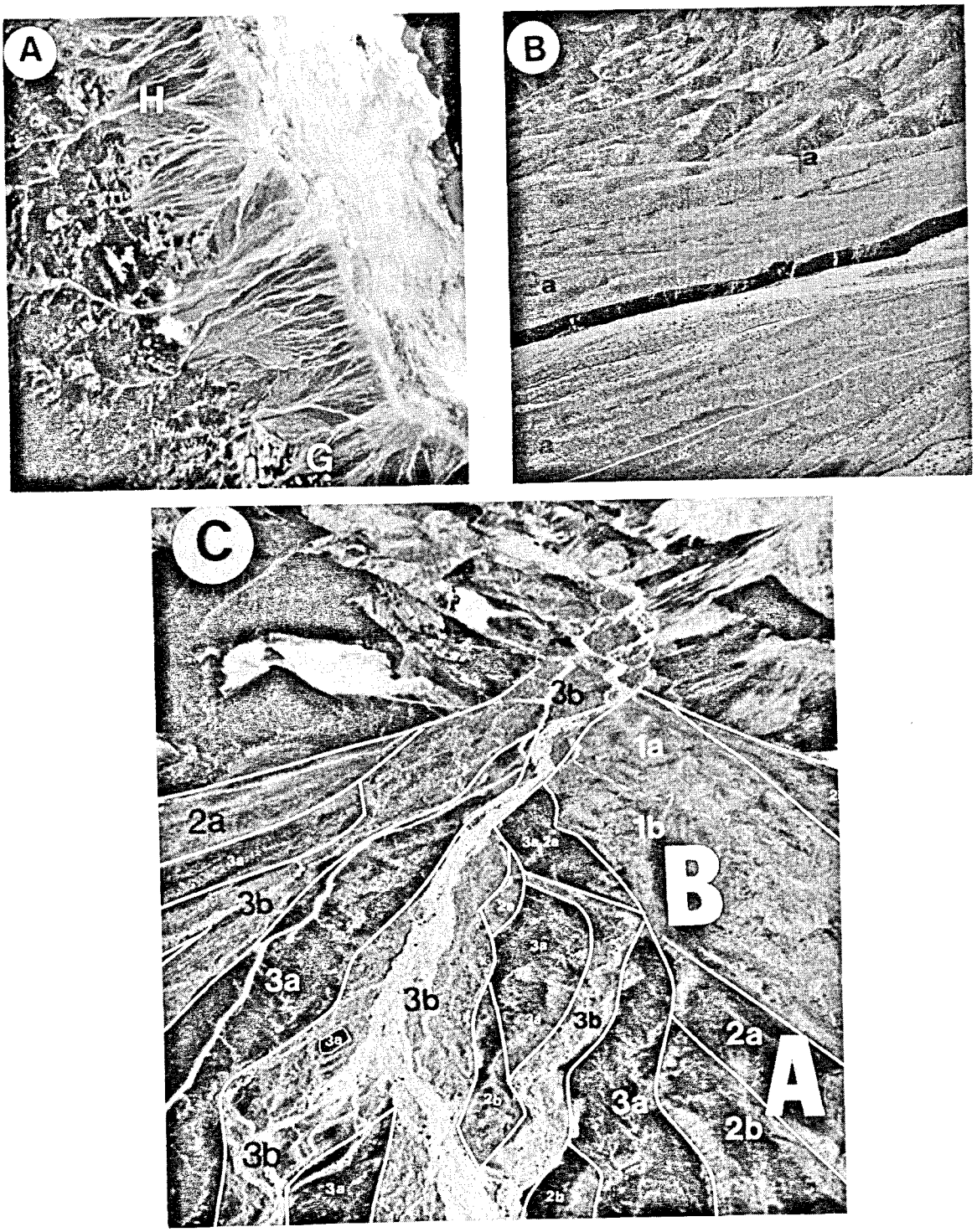

Figure 6. Sites of collection of alluvial-fan boulders in Death Valley. (A) Panchromatic SPOT image of southern Death Valley, showing the positions of Hanuapah Canyon fan (H) and Galena Canyon fan (G) on the bajada debouching from the east side of the Panamint Range. Width of image about 45 km. (B) Oblique aerial photograph of the head of Hanuapah fan, showing the locations of boulder collection from units 1a, 2a and 3a. (C) Oblique aerial photograph of the top of Galena Canyon fan. Letter A is the location of the sample from the 2a unit (apparent age 318 ± 12 ka), and letter B is the location of the sample from the 1b unit (apparent age 320 ± 14 ka). Mapped units correspond to Dorn (1988)

The Q1a unit of Hanaupah Canyon and Q1b unit of Hanaupah Canyon show minimum exposure ages of ~300 ka. These are similar to the ages obtained for the older units at Galena Canyon fan, despite the very different tectonic setting that resulted in a knife-like ridge for Hanaupah Q1b (Figure 6B) and a low ballena for Galena Q1b and Q2a (Figure 6C). We suspect that some sort of equilibrium condition may be in effect, where relatively slow rates of calcrete erosion may result in an apparent age of ~300 ka. Again the total elapsed interval is bounded by a $^{26}Al/^{10}Be$ ratio close to 6.

These results point to future tests. For example, cobbles from the active channel of Hanaupah Canyon fan and from a position at depth have been collected in order to assess net variability in the prior exposure history of alluvial-fan clasts. Exposed bedrock and colluvium at different elevations and different positions in the Panamint Range have been collected to assess detailed questions on how long material is exposed as bedrock, as opposed to colluvium. An analysis of multiple nuclides in depth profiles on older alluvium would assess if the surface of a 'stable desert pavement' is eroding, and how fast.

Case study of marine terraces

Samples were collected from two marine terraces at Punta Caballos in southern Peru (Figure 7). This is an extremely arid region. We would expect that the cobbles exposed at the surface of a marine terrace have experienced a complex history of hillslope exposure, slope transport, perhaps fluvial transport to the coast, littoral transport, and eventually tectonic uplift and isolation from waves. Surface cobbles were collected from a desert pavement at this site. However, the cobbles have no rock varnish for comparison, due to aeolian abrasion removing the weaker varnish.

The ^{10}Be–^{26}Al ages for the lowest marine terrace and a higher terrace (Table II) are difficult to interpret. At face value, the age for the lower terrace would be consistent with an interglacial terrace formed during oxygen isotope stage 5 and the higher terrace formed perhaps during an earlier interglacial. However, the $^{26}Al/^{10}Be$ ratios plot below the erosion island in Figure 2, suggesting that substantial periods of burial had occurred. Similarly, marine terrace samples from South Carolina also have low $^{26}Al/^{10}Be$ ratios (see Upland

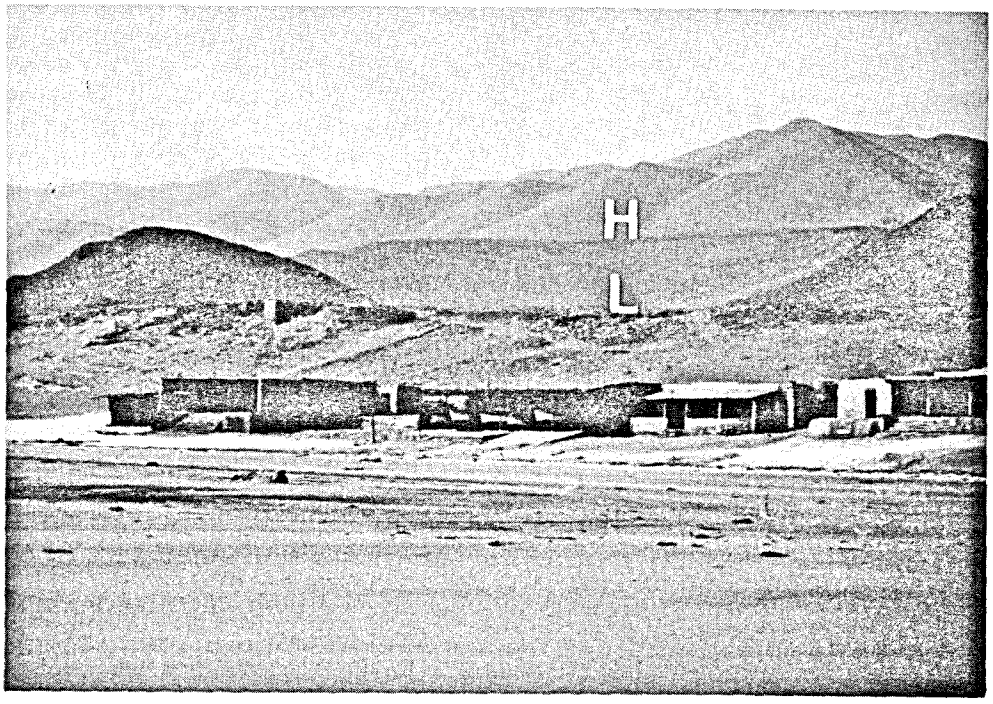

Figure 7. Sites of collection of clasts on marine terraces from southern Peru. Letter L identifies the lower and letter H the higher of the two terraces that were sampled

Table V. Cosmogenic nuclide accumulations in selected sand (paper in preparation) and loess samples

Site	Measured concentrations (10^6 atom/g SiO_2)		Effective exposure ages (ka)	
	^{10}Be	^{26}Al	^{10}Be	^{26}Al
Sand				
Ogolien, Sahara	0·42 ± 0·02	1·78 ± 0·13	100	70
Ogolien, Sahara	0·43 ± 0·03	1·70 ± 0·07	105	70
Modern Dune, Sahara	0·45 ± 0·02	1·63 ± 0·06	110	67
Gran Desierto, Mexico	0·41 ± 0·02	1·99 ± 0·13	71	58
Gobabeb, Namibia	0·56 ± 0·03	1·18 ± 0·03	105	36
Loess				
Banks Penninsula-1 New Zealand	0·05 ± 0·01	0·30 ± 0·10	9	9
Banks Penninsula-4 New Zealand	0·04 ± 0·01	0·55 ± 0·07	7	15
Kaiserstuhl Germany	0·03 ± 0·01	0·40 ± 0·15	4	9

Unit in Table II). Gravel from a clay matrix was sampled from the Upland Unit, a marine deposit about 3 m thick that is thought to be Miocene in age, perhaps Oligocene (D. J. Colquhoun, personal communication). In this particular circumstance, the exposure history of the sampled gravels is difficult to reconstruct.

The difficulty in obtaining suitable material for dating landforms in such hyper-arid regions and these intriguing ages certainly warrant further examination with stable cosmogenic nuclides, including a more detailed collection of cobbles from the current sea shore and from depth in the terrace covers.

Case study of aeolian deposits (sand dunes and loess)

The five samples from sand dunes show a consistent ^{10}Be–^{26}Al exposure age pattern, of ~70–100 ka (Table V, paper in preparation). ^{10}Be exposure ages are about 20 per cent higher than those based on ^{26}Al. The consistently low $^{26}Al/^{10}Be$ ratios (2–4) compared to the ratio of 6 at production in the Sierra Nevada glacial polish clearly indicates that the principal cause of lowering of the ratio is not continued irradiation at or near the surface. All these data are consistent with repeated cycles of near-surface exposure, followed by burial at depth.

A scenario of reburial and re-exposure for hundreds of thousands of years is what would be expected of quartz collected from ergs. However, these are the first direct measurements to test this intuitively logical model. We are in the process of refining the nuclear method of assessing the history of grains in sand dunes. By using ^{26}Al and ^{10}Be with long half-lives, *in situ* ^{14}C with a short half-life, and the stable nuclide ^{21}Ne, we should be able to further constrain the exposure history of aeolian sands. Furthermore, by sampling bedrock surfaces directly underneath dunes, we hope to constrain the length of time sand has covered a site.

Samples of glacially derived loess from the Banks Peninsula in New Zealand and the Kaiserstuhl near Freiberg in the Rhine Valley of Germany give apparent exposure ages that are mid to early Holocene (Table V). The components of the exposure history of the loess may include; prior to incorporation in a glacier; in a proglacial position; in intermediate depositional positions; and exposure at the collection site. It is likely that the New Zealand loess has a modern component (Taylor *et al.*, 1983), raising the intriguing possibility of using modern loess to assess the exposure history of the constituents of glacial flour.

CONCLUSION

Cosmogenic nuclides are not simply a one-number surface exposure dating method, but rather a set of tools to study geomorphic processes on timescales truly appropriate to the development of most landscapes. The

set includes stable (^{3}He, ^{21}Ne) and the short-lived nuclides (e.g. ^{14}C) appropriate for the study of Holocene landscapes. Forms that have evolved during the Quaternary can be investigated by ^{10}Be, ^{26}Al, ^{36}Cl, ^{41}Ca and the stable nuclides. The long-lived nuclides, ^{10}Be, ^{53}Mn and ^{129}I should open windows into Tertiary landscapes.

Cosmogenic nuclides provide 'dwell' times for material now exposed at the surface, because they integrate time in a surface layer that is about 0·5 m thick. They can be used for a variety of process studies: (i) for dating bedrock surfaces created by erosional processes, where the surface does not have a prior history of exposure to cosmic rays; (ii) for dating depositional landforms, if the clasts have not had a prior exposure history; (iii) for understanding the history of a landform that has been buried, which is especially useful where no materials are available for dating in a stratigraphic context; (iv) to constrain the long-term geomorphic history of clasts with complex histories of exposure, burial and re-exposure; and (v) for providing rates of erosion of bedrock.

The challenge is to see the potential of cosmogenic nuclides as being more than just a dating method. To meet this challenge, geomorphologists may have to rethink and create innovative tests of some long-held assumptions about how landscapes evolve.

ACKNOWLEDGEMENTS

We thank T. Cerling, D. J. Colquhoun, J. Hawkins, G. Teying, M. Xingyuan for providing rock samples; G. Kocurek, N. Lancaster, H. Lange, M. K. Seeley for sand samples; and S. M. McLennan and S. R. Taylor for loess samples. We also thank D. Matriano for part of the sample preparation. This work was supported by NSF Grant EAR 89-04677 and NASA Grant NAG 9-33. Field collection expenses supported in part by NSF PYI (Dorn).

REFERENCES

Bach, A., Elliott-Fisk, D. L., Liu, T., Dorn, R. I., Phillips, F. M. and Zreda, M. 1991. 'Pleistocene glacial moraine complexes at Pine and Bishop Creeks, east-central Sierra Nevada, CA', *Geological Society of America Abstracts with Program*, **23**(5), 223–224.

Bateman, P. C. 1965. 'Geology and Tungsten Mineralization of the Bishop District, California', *U.S. Geological Survey Professional Paper*, **470**.

Berry, M. 1991. 'Soil-geomorphic analysis of late-Quaternary glaciation, eastern escarpment of the central Sierra Nevada, California', *Geological Society of America Abtracts with Program*, **23**(5), 99–100.

Cerling, T. E. 1990. 'Dating geomorphic surfaces using cosmogenic He-3', *Quaternary Research*, **33**, 148–156.

Craig, H. and Poreda, R. J. 1986. 'Cosmogenic ^{3}He in terrestrial rocks: the summit lavas of Maui', *Proceedings of the National Academy of Science U.S.A.*, **83**, 1970–1974.

Davis, R. J. and Schaeffer, O. A. 1955. 'Chlorine-36 in nature', *Annals New York Academy Science*, **62**, 105–122.

Dorn, R. I. 1988. 'A rock varnish interpretation of alluvial-fan development in Death Valley, California', *National Geographic Research*, **4**, 56–73.

Dorn, R. I. 1989. 'Cation-ratio dating of rock varnish: A geographical perspective', *Progress in Physical Geography*, **13**, 559–596.

Dorn, R. I. and Krinsley, D. H. 1991. 'Cation-leaching sites in rock varnish', *Geology*, **19**, 1077–1080.

Dorn, R. I. and Phillips, F. M. 1991. 'Surface exposure dating: review and critical evaluation', *Physical Geography*, **12**, 303–333.

Dorn, R. I., Turrin, B. D., Jull, A. J. T., Linick, T. W. and Donahue, D. J. 1987. 'Radiocarbon and cation-ratio ages for rock varnish on Tioga and Tahoe morainal boulders of Pine Creek, eastern Sierra Nevada, and paleoclimatic implications', *Quaternary Research*, **28**, 38–49.

Dorn, R. I., Jull, A. J. T., Donahue, D. J., Linick, T. W. and Toolin, L. J. 1989. 'Accelerator mass spectrometry radiocarbon dating of rock varnish', *Geological Society of American Bulletin*, **101**, 1363–1372.

Dorn, R. I., Cahill, T. A., Eldred, R. A., Gill, T. E., Kusko, B., Bach, A. and Elliott-Fisk, D. 1990. 'Dating rock varnishes by the cation ratio method with PIXE, ICP, and the electron microprobe', *International Journal of PIXE*, **1**, 157–195.

Dorn, R. I., Clarkson, P. B., Nobbs, M. F., Loendorf, L. L. and Whitley, D. S. 1992. 'Radiocarbon dating inclusions of organic matter in rock varnish, with examples from drylands', *Annals of the Association of American Geographers*, **82**, 136–151.

Elmore, D. and Phillips, F. M. 1987. 'Accelerator mass spectrometry for measurement of long-lived radioisotopes', *Science*, **236**, 543–550.

Graf, T., Kohl, C. P., Marti, K. and Nishiizumi, K. 1990. 'Cosmic-ray produced Ne in Antarctic rocks', *Geophysical Research Letters*, **18**, 203–206.

Harvey, A. M. 1989. 'The occurrence and role of arid zone alluvial fans', in Thomas, D. S. G. (Ed.), *Arid Zone Geomorphology*, Belhaven Press, London, 136–158.

Hooke, R. L. and Lively, R. S. 1979. *Dating of Quaternary deposits and associated tectonic events by U/Th methods, Death Valley, California*, Final Report for NSF Grant EAR 79-19999, 21 pp.

Jull, A. J. T., Donahue, D. J., Linick, T. W. and Wilson, C. G. 1989. 'Spallogenic carbon-14 in high altitude rocks and in Antarctic meteorites', *Radiocarbon*, **31**, 719–724.

Klein, J., Middleton, R. and Tang, H. 1982. 'Modifications of an FN tandem for quantitative Be-10 measurement', *Nuclear Instruments Methods in Physics Research*, **193,** 601–616.
Kohl, C. P. and Nishiizumi, K. 1992. 'Chemical isolation of quartz for measurement of *in situ* produced cosmogenic nuclides', *Geochimica et Cosmochimica Acta*, **52,** 3583–3587.
Kurz, M. 1986. 'In situ production of terrestrial cosmogenic helium and some applications to geochronology', *Geochimica et Cosmochimica Acta*, **50,** 2855–2862.
Lal, D. 1988. 'In situ—produced cosmogenic isotopes in terrestrial rocks', *Annual Review Earth Planetary Science*, **16,** 355–388.
Lal, D. 1991. 'Cosmic ray labeling of erosion surfaces: in situ nuclide production rates and erosion models', *Earth and Planetary Science Letters*, **104,** 424–439.
Lal, D. and Arnold, J. R. 1985. 'Tracing quartz through the environment', *Proceedings Indian Academy Science (Earth Planetary Science)*, **94,** 1–5.
Lal, D. and Peters, B. 1967. 'Cosmic ray produced radioactivity on the earth', *Handbuch der Physik*, Springer-Verlag, Berlin, **46/2,** 551–612.
Lal, D., Nishiizumi, K. and Arnold J. 1987. 'In situ cosmogenic ^{3}H, ^{14}C and ^{10}Be for determining the net accumulation and ablation rates of ice sheets', *Journal of Geophysical Research*, **92,** 4947–4952.
Marti, K. and Craig, H. 1987. 'Cosmic-ray produced neon and helium in the summit lavas of Maui', *Nature*, **325,** 335–337.
Meek, N. 1989. 'Geomorphic and hydrologic implications of the rapid incision of Afton Canyon, Mojave Desert, California', *Geology*, **17,** 7–10.
Middleton, R., Klein, J., Raisbeck, G. M. and Yiou, F. 1983. 'Accelerator mass spectrometry with Al-26', *Nuclear Instruments Methods in Physics Research*, **218,** 430–438.
Nishiizumi, K., Lal, D., Klein, J., Middleton, R. and Arnold, J. R. 1986. 'Production of Be-10 and Al-26 by cosmic rays in terrestrial quartz in situ and implications for erosion rates', *Nature*, **319,** 134–136.
Nishiizumi, K., Winterer, E. L., Kohl, C. P., Klein, J., Middleton, R., Lal, D. and Arnold, J. R. 1989. 'In situ Be-10 and Al-26 in granitic rocks with glacially polished surfaces', *Journal of Geophysical Research*, **94,** 17907–17915.
Nishiizumi, K., Kohl, C. P., Arnold, J. R., Klein, J., Fink, D. and Middleton, R. 1991a. 'Cosmic ray produced Be-10 and Al-26 in Antarctic rocks: exposure and erosion history', *Earth and Planetary Science Letters*, **104,** 440–454.
Nishiizumi, K., Kohl, C. P., Shoemaker, E. M., Arnold, J. R., Klein, J., Fink, D. and Middleton, R. 1991b. 'In Situ Be-10 Al-26 exposure ages at Meteor Crater, Arizona', *Geochimica et Cosmochimica Acta*, **55,** 2699–2703.
Nishiizumi, K., Kohl, C. P., Arnold, J. R., Caffee, M. W., Finkel, R. C., Southon, J., Shoemaker, E. M. and Shoemaker, C. S. 1992. 'Exposure histories of desert sands using *in situ* produced cosmogenic nuclides', *EOS*, **73,** 185.
Phillips, F. M., Leavy, B. D., Jannik, N. O., Elmore, D. and Kubik, P. W. 1986. 'The accumulation of cosmogenic chlorine-36 in rocks: a method for surface exposure dating', *Science*, **231,** 41–43.
Phillips, F. M., Zreda, M. G., Smith, S. S., Elmore, D., Kubik, P. W., Dorn, R. I. and Roddy, D. 1991. 'Age and geomorphic history of Meteor Crater, Arizona from cosmogenic Cl-36 and C-14 in rock varnish', *Geochimica et Cosmochimica Acta*, **55,** 2695–2698.
Stadelman, S. 1989. *Pedogenesis and geomorphology of Hanaupah Canyon alluvial fan, Death Valley, California*, M.S. Thesis, Texas Tech. Univ.
Taylor, S. R., McLennon, S. M. and McCulloch, M. T. 1983. 'Geochemistry of loess, continental crustal composition and crustal model ages', *Geochimica et Cosmochimica Acta*, **47,** 1897–1905.
Young, R. W. 1983. 'The tempo of geomorphological change: evidence from southeastern Australia', *Journal of Geology*, **91,** 221–230.
Zreda, M. G., Phillips, F. M., Elmore, D., Kubik, P. W., Sharma, P. and Dorn, R. I. 1991. 'Cosmogenic chlorine-36 production rates in terrestrial rocks', *Earth and Planetary Science Letters*, **105,** 94–109.